PAPER

Design and synthesis of potent *N*-phenylpyrimidine derivatives for the treatment of skin cancer†

Udit J. Chaube, Vivek K. Vyas and Hardik G. Bhatt*

The development of novel synthetic compounds for the treatment of skin cancer is much needed, as there is a sudden rise in the incidence of skin cancer throughout the world and the available chemotherapy is facing problems of resistance. Hence, present research efforts have been made to discover potent molecules against skin cancer. Pharmacophore models were developed using the GALAHAD module of Sybyl X, followed by validation, virtual screening, design and *in silico* ADMET studies. Based on features generated in the computational studies and the structural importance of the pyrimidine moiety with the highest Q_{FIT} value molecule for virtual hits; it was selected as a core moiety for further designing molecules of interest. Fourteen substituted pyrimidine derivatives were designed, synthesized and characterised by ^{1}H and ^{13}C NMR, mass and elemental analysis, while the purity was checked by HPLC. All these compounds were evaluated in *in vitro* studies on five cancer lines; from which, four compounds were found to be potent, specifically with the skin cancer cell line. Based on the results of the *in vitro* studies, they were selected further, along with **5-FU**, for an *in vivo* study with the DMBA-induced skin cancer model. One compound, **6h**, showed favourable action against skin cancer and treated tumours, demonstrating the potential of the series. This study could be explored in future to design lead molecule for the treatment of skin cancer.

1. Introduction

Cancer is a disease with an uncontrolled proliferation of cells and a big potential for it to invade to any part of the body. Cancer is one of the leading causes of death in the world and the second most common disease after cardiovascular disorders.[1] It is predicted that by the end of the year 2020, approximately 16.5 million new cases will be detected, and most of them will be from developing countries.[1] Various preventive measures are now available for the treatment of cancers, but a few cancers, such as skin cancer, have no preventive measures. A WHO report of world cancer reported that skin cancer constitutes nearly 30% of all recently diagnosed cancers in the world.[1–3] Difficulties associated in the treatment of skin cancer include the resistance to existing chemotherapy due to the presence of survivin molecules in the cells.[2] A few cytotoxic drugs are available for the treatment of skin cancer; however, they exhibit

Department of Pharmaceutical Chemistry, Institute of Pharmacy, Nirma University, S. G. Highway, Chharodi, Ahmedabad 382 481, India. E-mail: hardikbhatt23@hotmail. com; Fax: +91 2717 241916; Tel: +91 79 30642727

toxic effects on the kidneys, lungs, heart, brain and gastrointestinal tract.[4] If skin cancer cannot be diagnosed at an early stage, then it can metastasized to various parts of the body through the lymph system and blood circulation. UV radiation is mainly responsible for the development of skin cancer[5,6] through direct and indirect mechanisms like immune suppression, the formation of cyclobutane pyrimidine dimers, p53 gene mutation, oxidative stress, *etc.*[7–9] Another factor responsible for the skin cancer is having a fair complexion due to the deficiency of the UV-blocking pigment known as eumelanin.[9] Ozone layer depletion, altitude, latitude and weather conditions also affect the intensity of UV radiation. The rudimentary mechanism behind the pathogenesis of skin cancer due to UV radiation is a dented DNA, which results in the formation of an assembly of bad cells[4,8] and the end result of this is the formation of a tumour. Normally, the p53 protein triggers the p21 protein and this intrudes the cell cycle in between the G1 and S phases. Due to the mutation in the p53 protein, this normal process get disturbed, which upshots into the copious growth of defective cells, ultimately resulting in skin cancer. Hence, the development of novel chemical compounds for the treatment of skin cancer is a desirable goal of this work. Herein, efforts were made to design novel pyrimidine derivatives *via* a pharmacophore-based scaffold hopping method. The designed molecules were synthesised and evaluated against different cancer cell lines, including the skin cancer cell line (A-375). Potent compounds in the *in vitro*

evaluation were further evaluated by *in vivo* evaluation with the DMBA-induced skin cancer animal model.

2. Results and discussion

2.1 Rational for design of the compounds

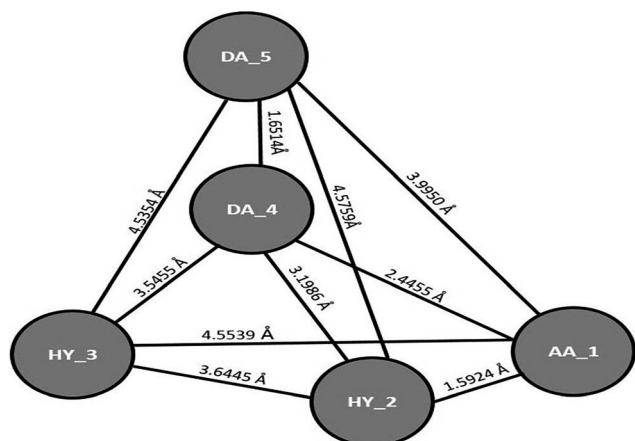The involvement of CDK2 in skin cancer *via* p53 and p21 proteins is well known, therefore in this study, eight molecules (1–8), (Table ST-1, ESI†) were taken from the published literature[10–15] for the generation of pharmacophore models. Twenty pharmacophore models were generated through the GALAHAD module of Sybyl X;[16] among them, model-15 (Table ST-2, ESI†) was selected as the best model based on having the lowest energy value, maximum number of hits and a comparatively high specificity value.[17–20] A 2D representation of model-15 is shown in Fig. 1 (a 3D-representation is shown as Fig. SF-1, ESI†), which consisted of 2 donor atoms, 2 hydrophobic sites and 1 acceptor atom. Validation of the best pharmacophore model was carried out by the GH (Guner Henry) scoring method and ROC (Receiver Operating Characteristics) curve analysis to check the accuracy and reliability of the model.[21–23] The GH score and the area under curve (AUC) of the ROC curve analysis of model-15 were 0.703 and 0.7, respectively (Tables ST-3 and ST-4, ESI†). Pharmacophore model-15 was also used as a 3D search query against the NCI database, which consists of 250 000 diverse anticancer molecules. Compounds having various chemical groups spatially overlapping (map) with the corresponding features of pharmacophoric model 15 were captured as hits, with a Q_{FIT} value. The retrieved hit NCIIDM81922 with the highest Q_{FIT} value of 93.18 consisted of a pyrimidine ring as the core moiety in the structure (the structures of the top five hit molecules and their Q_{FIT} values are given in the ESI†).

Fig. 1 2D representation of the best pharmacophore model generated through GALAHAD module of Sybyl X.
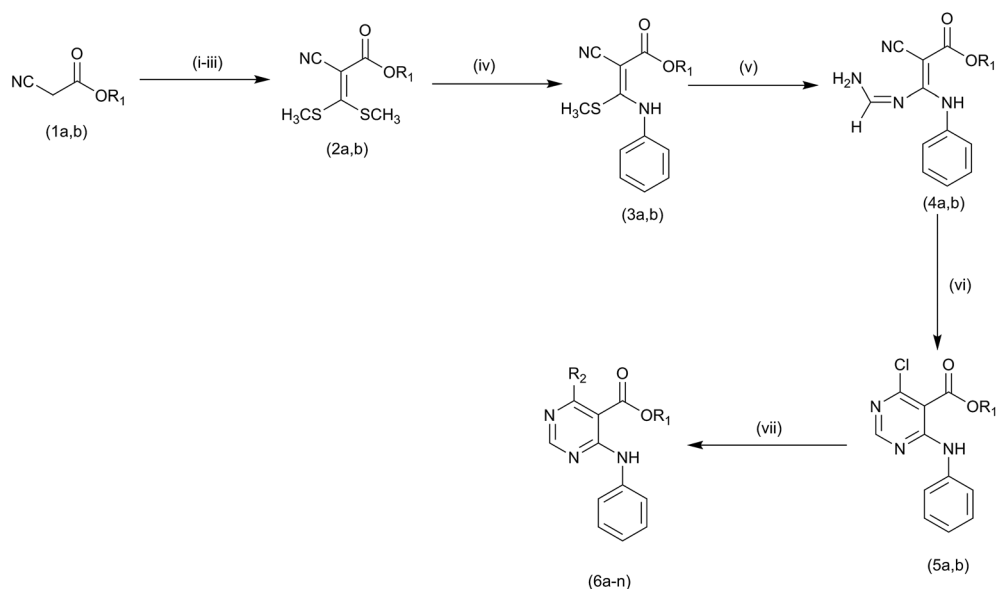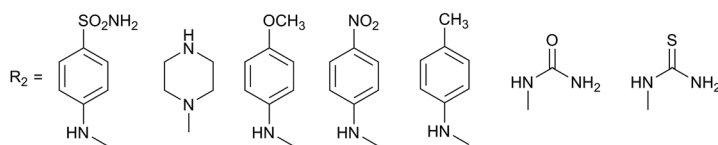
Scheme 1 Reagents and conditions: (i) aqueous KOH, DMF, stirring with cooling for 10 min; (ii) carbon disulphide, stirring at 25 °C for 1 h; (iii) dimethyl sulphate, stirring at 0 °C; (iv) aniline, ethanol, reflux for 2 h; (v) formamidine acetate in ethanolic NaOH, stirring at 0–5 °C for 6 h; (vi) 1,4-dioxane saturated with HCl, stirring for 24 h; and (vii) aromatic/aliphatic amines, IPA, a few drops of concentrated HCl, reflux for 2–6 h.

N-Phenylpyrimidine was selected as a core moiety for the design of compounds based on their maximum similarity with the generated pharmacophore. Another advantage associated with the selection of the *N*-phenylpyrimidine ring is the presence of a pyrimidine ring, which is similar to the most effective marketed drug available for the treatment of skin cancer (5-fluorouracil (**5-FU**)). Based upon these facts and the results of the pharmacophore modelling, fourteen novel derivatives were designed and synthesized (**6a–n**) (Scheme 1). In the designed series, different substitutions were carried out at the R_1 (**C-5**) and R_2 (**C-4**) positions of the *N*-phenylpyrimidine ring. Two different series were prepared by using two different starting materials: methylcyanoacetate and ethylcyanoacetate, which resulted in methyl and ethyl substitution at the R_1 position of the *N*-phenylpyrimidine moiety. Different aliphatic and aromatic amines were substituted at the R_2 position to check the effects of the additional hydrophobic group on the skin cancer activity. The designed compounds were predicted for their *in silico* toxicity risk prediction parameters. The factors of toxicity risk management are mutagenicity, tumorigenicity, irritant effect and reproductive effect. Results of the toxicity prediction study revealed that four compounds, namely **6f**, **6g**, **6m**, and **6n**, were at risk of mutagenic toxicity; while compounds **6g** and **6n** showed a tumorigenic effect and compounds **6f** and **6m** showed an irritant effect. All the other compounds were non-toxic (Table ST-5, ESI†).

3. Chemistry

Our previously reported synthetic scheme[24] was utilised as a reference for the synthesis of intermediates and target compounds. As shown in Scheme 1, methyl or ethyl-substituted *S*,*S*-acetal (**2a,b**) was afforded from methylcyanoacetate or ethylcyanoacetate, respectively, by reacting with carbon disulphide in the presence of base potassium hydroxide (step-I). Step-II involved the nucleophilic displacement of one –SCH₃ group from *S*,*S*-acetal (**2a,b**) by aniline, which resulted in the formation of methyl- or ethyl-substituted *S*,*N*-acetal (**3a,b**). Step-II's

product (**3a,b**) was treated with formamidine acetate in the presence of sodium hydroxide and ethanol to afford product (**4a,b**), which was cyclised to give pyrimidine moiety (**5a,b**) in the presence of HCl-saturated dioxane. HCl is known to enhance the reactivity of the –CN group, which resulted in the formation of 5-substituted-6-(*N*-phenyl)-4-chloropyrimidine (**5a,b**) as a core moiety. This core moiety was utilised for the synthesis of the designed compounds as shown in Scheme 1. Chlorine on the pyrimidine ring was a point for nucleophilic substitution by different amines. Seven different aliphatic as well as aromatic amines were substituted on the pyrimidine moiety to afford 14 different final compounds (**6a–n**).

The chemical structure of all the compounds was confirmed by ^{1}H and ^{13}C NMR, mass spectral and elemental analysis data. The purity of the compounds were determined from HPLC analysis (Table ST-6, ESI†). The significant features of the ^{1}H NMR spectra include the appearance of different sets of hydrogen atom resonances, corresponding to the protons in the aromatic rings (on **C-4** and **C-6** of pyrimidine), pyrimidine ring (at **C-2**), secondary amines (on **C-4** and **C-6** of pyrimidine), methyl and ethyl groups (as R_1). For the synthesized compounds, the set of protons corresponding to the aromatic ring appear in the range of 6.50–8.00 δ ppm, showing the expected multiplicity and integration values. The resonance peaks, in the region from 8.01 to 8.70 δ ppm, correspond to the pyrimidine proton. The Ar-H of the ^{1}H NMR spectrum correlate with C atoms from 110–170 δ ppm in the ^{13}C NMR spectra. Signals for the secondary amine proton (–NH–) appear as a singlet in the region of 8–11 δ ppm. For the –CH₃ group of methyl acetate, a singlet appears from 3.00 to 3.90 δ ppm. For the –CH₃ of ethyl acetate, a triplet appears in the region of 1.20–1.40 δ ppm and for the –CH₂ group of ethyl acetate, a quartet appears in the region of 4.13–4.94 δ ppm (the ^{1}H NMR, ^{13}C NMR and mass spectra of a few representative compounds are provided in the ESI†). The crystal structure of compound **6h** was derived by single crystal X-ray analysis and is shown in Fig. 2 (detailed descriptions of the results of the X-ray crystallography studies are provided in the ESI†).
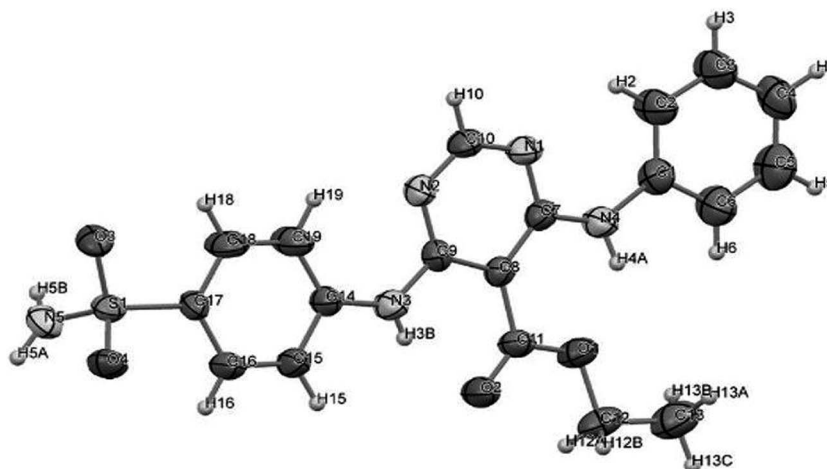

Fig. 2   Determination of structure of compound **6h** by X-ray crystallographic studies.

4. Biological evaluation

4.1 Antiproliferative *in vitro* assay

Synthesized derivatives were screened against five different cancer cell lines, namely A-375, MCF-7, DU-145, HEP-3B and the non-cancerous cell line VERO, and their IC_{50} values are reported in Table 1. A few compounds showed potent activity with various cell lines. Compounds **6a** (IC_{50} = 0.0073 μM), **6h** (IC_{50} = 0.0047 μM), **6j** (IC_{50} = 0.0079 μM) and **6k** (IC_{50} = 0.0876 μM) showed potent activity with the skin (melanoma) cancer cell line, A-375. Compounds **6h** (IC_{50} = 0.0075 μM), **6j** (IC_{50} = 0.0042 μM) and **6n** (IC_{50} = 0.016 μM) showed potent activity with the breast cancer cell line MCF-7. Compounds **6h** (IC_{50} = 0.0222 μM), **6k** (IC_{50} = 0.0561 μM), **6l** (IC_{50} = 0.018 μM) and **6m** (IC_{50} = 0.0302 μM) showed potent activity with the hepatoma cancer cell line HEP-3B. Compounds **6b** (IC_{50} = 0.0073 μM) and **6h** (IC_{50} = 0.0075 μM) showed potent activity with the prostate cancer cell line DU-145. In the case of the VERO cell line, compounds **6c**, **6d**, **6e**, **6i** and **6l** were found cytotoxic with the normal VERO cell line, while the rest of the compounds were found to be non-toxic, showing IC_{50} values > 500 μM. **5-FU** showed IC_{50} values of 0.0042 μM (on A-375), 1.60 μM (on MCF-7), 1.75 μM (on HEP-3B) and 0.07 μM (on DU-145). From the results of the *in vitro* activity of the synthesized compounds, it was found that the synthesized compounds showed the most prominent activity on the skin cancer cell line (A-375). Hence, the highest active compounds, **6a**, **6h**, **6j** and **6k**, were further selected for *in vivo* evaluation in Swiss-albino mice with the DMBA-induced skin cancer model.

4.2 *In vivo* assay

An *in vivo* study was carried out in Swiss-albino mice with the 16 weeks DMBA-induced skin cancer model. Serum biomarkers and oxidative stress parameter levels were checked 12 weeks after the induction of skin cancer in the disease-induced mice. A significant increase (p < 0.05) in the serum level of the biomarkers, namely gamma glutamyl transferase (GGT), lactate dehydrogenase (LDH), C-reactive protein (CRP), and the oxidative stress parameter, malondialdehyde (MDA), and a significant decrease in serum levels of the other oxidative stress parameters, namely reduced glutathione (GSH) and superoxide dismutase (SOD), were observed in skin-cancer-induced mice compared to the normal control mice group, which confirmed the presence of skin cancer. After treatment with the synthesized compounds (2%) and standard 5-fluorouracil (**5-FU**) (2%) from the 12th to 16th weeks, it was found that compound **6h** and **5-FU** significantly reduced (p < 0.05) the levels of GGT, LDH, CRP (Fig. 3A–C) and MDA (Fig. 4A); while, it increased the levels of GSH and SOD (Fig. 4B and C) at the end of the 16th week which demonstrated the good anticancer activity. Statistical results of the serum biomarkers and the oxidative stress parameter levels are shown in Tables 2 and 3, respectively. Tumour volume, tumour burden and survival rate were observed from the 6th to the 16th weeks after the induction of skin cancer, and the data are shown in Table 4. A significant increase (p < 0.05) in tumour volume and tumour burden were observed at the end of the 12th week in the disease (skin cancer)-induced mice group. The effect of the **5-FU** and synthesized compounds **6a**, **6h**, **6j** and **6k** on tumour volume and tumour burden was observed from the 12th to 16th week and it was found that at the end of 16th week, the highest reduction in tumour volume and tumour burden was noted in compound **6h** and **5-FU** (Fig. 5A and B). At the end of the study (16th week), no significant differences in serum biomarkers levels, oxidative stress parameters, tumour volume and tumour burden were observed between compound **6h** and the **5-FU** treated groups, which confirmed the anticancer activity of **6h**. A 100% survival rate was observed in the normal control group, and the skin cancer control group treated with **5-FU**, **6h** and **6j** from the 6th to the 16th week.

Table 1 *In vitro* antiproliferative activity of **5-FU** and synthesized compounds on various cancer cell lines

| Compounds	A-375 IC_{50} (μM)	MCF-7 IC_{50} (μM)	HEP-3B IC_{50} (μM)	DU-145 IC_{50} (μM)	VERO IC_{50} (μM)
5-FU	0.0042	1.60	1.75	0.07	>500
Series-1					
6a	0.0073	0.0101	2.5188	>100	>500
6b	0.1576	3.1948	0.239	0.0073	>500
6c	0.1443	0.0659	2.8571	>100	0.007
6d	0.4960	2.6525	>100	0.11	0.03
6e	1.5750	1.9007	3.0120	3.01	0.002
6f	0.6538	0.0548	3.4843	>100	>500
6g	5.615	0.0541	0.2240	>100	>500
Series-2					
6h	0.0047	0.0075	0.0222	0.0075	>500
6i	3.058	3.058	0.0386	>100	0.0121
6j	0.0079	0.0042	2.7472	2.7472	>500
6k	0.0876	0.0120	0.0561	25.8877	>500
6l	0.258	2.8735	0.018	2.8735	0.055
6m	0.95	3.8461	0.0302	3.6339	>500
6n	1.21	0.016	3.8314	0.9745	>500
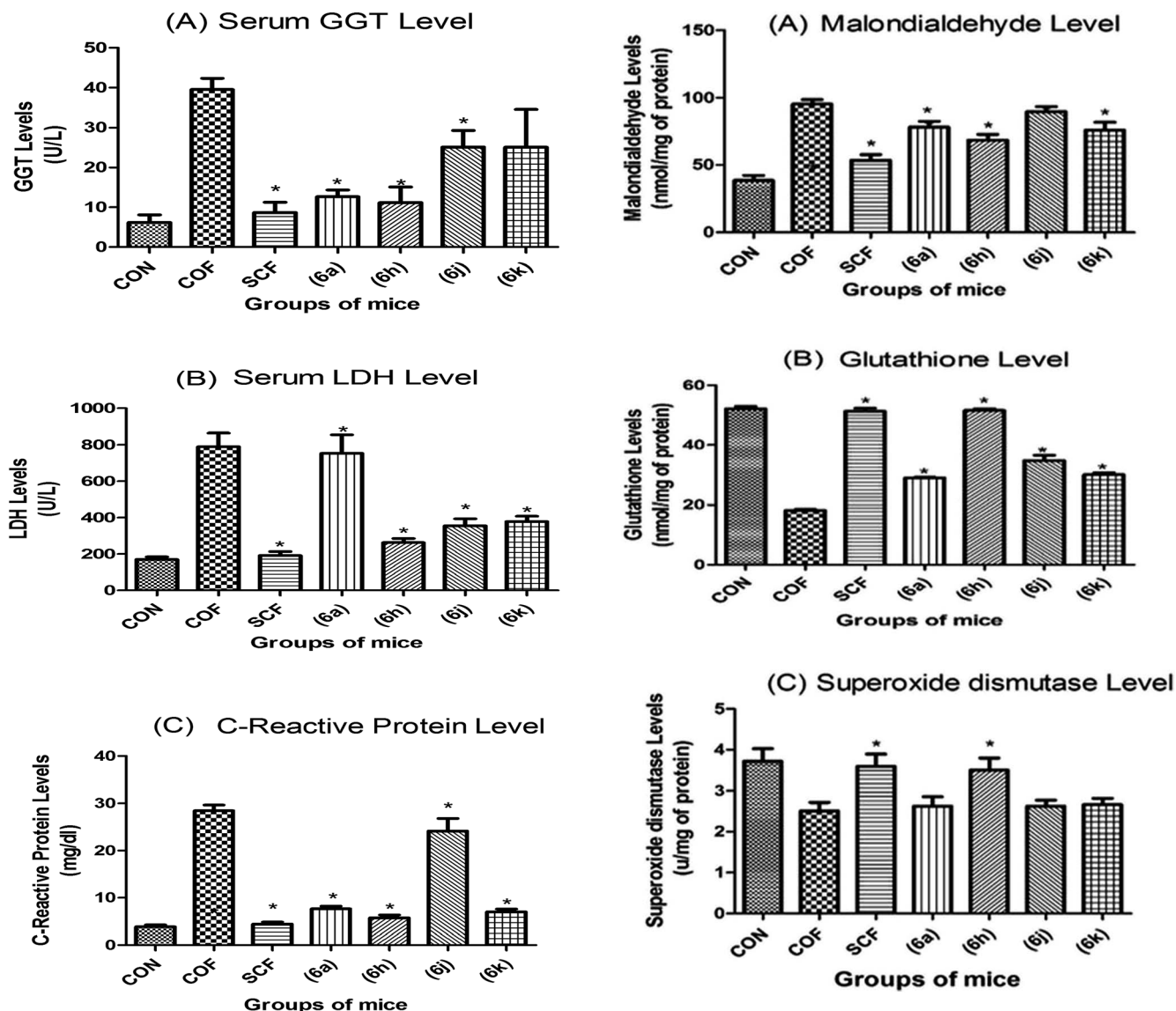
Fig. 3 Measurement of serum biomarkers after treatment with 5-FU and compounds 6a, 6h, 6j and 6k, where each bar represents mean ± SEM, $n = 6$ mice (Oneway ANOVA followed by Dunnett's multiple comparison test), * = $p < 0.05$ vs. normal control group: (A) gamma glutamyl transferase level; (B) lactate dehydrogenase level; (C) C-reactive protein level.

Fig. 4 Measurement of oxidative stress parameters after treatment with 5-FU and compounds 6a, 6h, 6j and 6k, where each bar represents mean ± SEM, $n = 6$ mice (Oneway ANOVA followed by Dunnett's multiple comparison test), * = $p < 0.05$ vs. normal control group: (A) malondialdehyde level; (B) glutathione level; (C) super oxide dismutase level.

Fig. 6(A)–(D) presents photographs of the caudal region of the skin of the mice and histopathological results of skin samples of the normal control group, skin cancer control group, skin cancer treated with 5-FU and skin cancer treated with compound 6h, respectively. Fig. 6A, i.e. the normal control group, presents the normal caudal region of the skin of the mice and histopathological section with various layers of skin. In the skin cancer control mice, photograph (Fig. 6B) shows that the generated tumour mass is thoroughly spread over the caudal region of the skin of the mice. The histopathological study also showed the disruption of the fatty layer with the presence of keratin pearls. The presence of rete ridges extending through the connective tissue was also seen, along with the marked
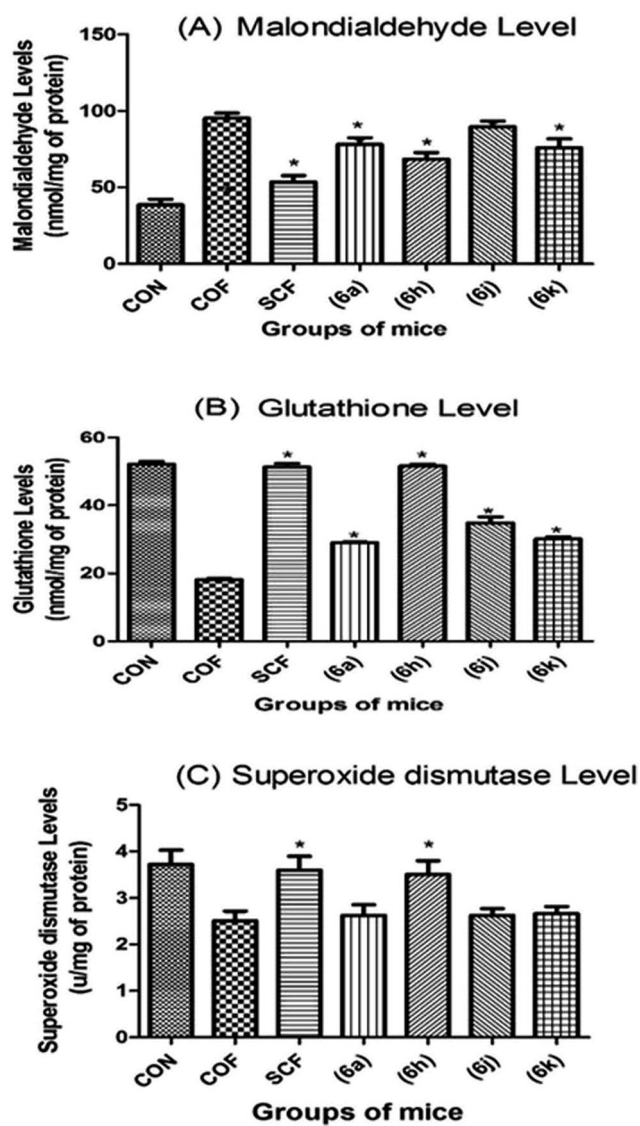
presence of dysplastic and hyperplastic epithelial cells. The photographs shown in Fig. 6C and D show that the tumour mass was completely removed from the caudal region of the skin of the mice treated with compound 6h and 5-FU. Histopathological sections of skin from mice treated with compound 6h and 5-FU showed the complete absence of keratin pearls, dysplastic epithelial cells or rete ridges, which proved the potency of 6h for the treatment (colour representation is given as Fig. SF-2†).

5. Structure activity relationship

A structure activity relationship study of synthesized compounds for their effectiveness on all four cell lines, namely

Table 2 Effect of 5-fluorouracil (2%) and compounds **6a**, **6h**, **6j**, and **6k** (2%) on serum levels of gamma glutamyl transferase (GGT), lactate dehydrogenase (LDH), C-reactive protein (CRP)[a]

Parameters	CON	COF	SCF	6a	6h	6j	6k
GGT (unit L^{-1})	6.17 ± 0.92	39.53 ± 0.82	8.68 ± 0.57	12.66 ± 0.43	11.19 ± 0.98	25.16 ± 0.97	25.12 ± 1.98
LDH (unit L^{-1})	170.6 ± 0.21	790.1 ± 1.53	191.7 ± 0.56	753.3 ± 1.91	262.7 ± 0.58	355.2 ± 0.62	378.7 ± 0.64
CRP (mg dL^{-1})	3.86 ± 0.28	28.44 ± 1.19	4.42 ± 0.22	7.66 ± 0.25	5.75 ± 0.27	24.14 ± 1.67	7.00 ± 0.20

[a] Each column represents mean $\pm$ SEM, $n = 6$ mice (Oneway ANOVA followed by Dunnett's multiple comparison test); GGT: gamma glutamyl transferase; LDH: lactate dehydrogenase; CRP: C-reactive protein; CON: normal control group; COF: skin cancer control group; SCF: skin cancer control group treated with **5-FU**.

Table 3 Effect of 5-fluorouracil (2%) and compounds **6a**, **6h**, **6j**, and **6k** (2%) on serum levels of malondialdehyde (MDA), reduced glutathione (GSH) and superoxide dismutase (SOD) levels[a]

Parameters	CON	COF	SCF	6a	6h	6j	6k
MDA (nmol mg^{-1})	38.46 ± 0.31	95.30 ± 0.35	53.42 ± 0.37	78.21 ± 0.36	68.38 ± 0.37	89.74 ± 0.32	75.80 ± 0.39
GSH (nmol mg^{-1})	52.13 ± 0.20	18.18 ± 0.19	51.32 ± 0.23	28.92 ± 0.12	51.60 ± 0.10	34.82 ± 0.31	30.07 ± 0.15
SOD (unit mg^{-1})	3.72 ± 0.48	2.51 ± 0.45	3.59 ± 0.43	2.62 ± 0.42	3.50 ± 0.49	2.62 ± 0.42	2.66 ± 0.42

[a] Each column represents mean $\pm$ SEM, $n = 6$ mice (Oneway ANOVA followed by Dunnett's multiple comparison test); MDA: malondialdehyde; GSH: reduced glutathione; SOD: superoxide dismutase; CON: normal control group; COF: skin cancer control group; SCF: skin cancer control group treated with **5-FU**.

Table 4 Effects of 5-fluorouracil (2%) and compounds **6a**, **6h**, **6j**, and **6k** (2%) on tumour volume, tumour burden and survival rate[a]

Groups treated with	Parameters	Number of weeks					
		6	8	10	12	14	16
CON	Tumour volume	0	0	0	0	0	0
	Tumour burden	0	0	0	0	0	0
	Survival rate	100%	100%	100%	100%	100%	100%
COF	Tumour volume	1.53	3.12	7.69	15.99	24.30	27.76
	Tumour burden	6.53	18.12	39.69	87.99	144.30	167.76
	Survival rate	100%	100%	100%	100%	83.33%	66.66%
SCF	Tumour volume	1.58	3.15	7.01	4.50	2.10	2.19
	Tumour burden	6.28	19.15	37.01	16.91	10.10	8.89
	Survival rate	100%	100%	100%	100%	100%	100%
6a	Tumour volume	1.46	3.97	7.80	8.14	7.14	6.10
	Tumour burden	6.46	20.97	40.80	32.54	26.64	24.05
	Survival rate	100%	100%	100%	83.33%	66.66%	66.66%
6h	Tumour volume	1.14	3.79	7.91	5.00	4.12	2.95
	Tumour burden	6.14	18.79	34.91	17.01	15.52	11.32
	Survival rate	100%	100%	100%	100%	100%	100%
6j	Tumour volume	1.13	3.16	7.70	6.34	5.11	4.31
	Tumour burden	6.13	19.16	38.70	24.64	19.61	16.31
	Survival rate	100%	100%	100%	100%	100%	100%
6k	Tumour volume	1.104	3.425	7.232	7.882	6.150	5.000
	Tumour burden	6.804	20.42	40.23	30.68	21.472	16.770
	Survival rate	100%	100%	100%	66.66%	50%	50%

[a] CON: normal control group; COF: skin cancer control group; SCF: skin cancer control group treated with **5-FU**.

skin cancer, breast cancer, hepatoma cancer and prostate cancer was carried out and is discussed in this section.

R_1 substitution of the pyrimidine ring was substituted with methyl as well as ethyl groups to check the effect of bulkiness on the activity against the skin cancer cell line. Compounds with methyl substitution at the R_1 position resulted in lower activity as compared to the ethyl-substituted compounds, which clearly indicated that groups with a higher carbon number, like ethyl, or at a higher R_1 position are required to increase the potency of the synthesized compounds. Apart from the highest active
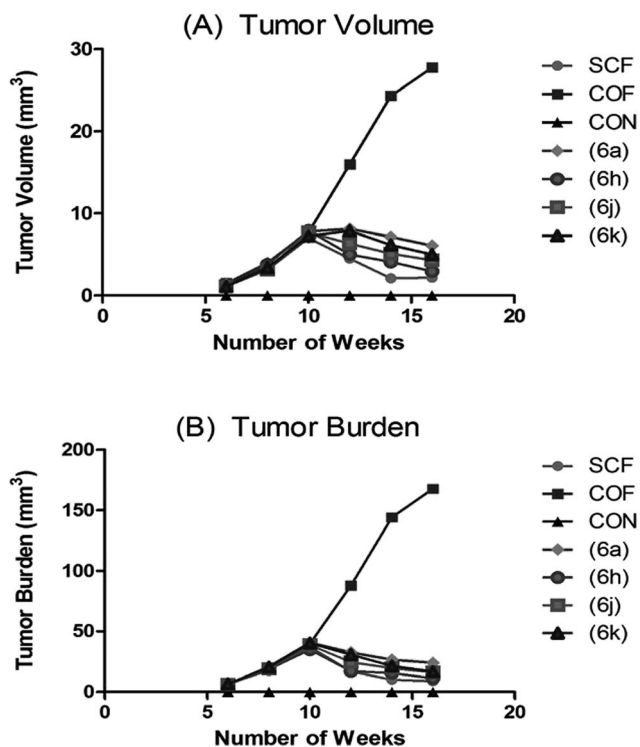
Fig. 5 Comparison of the growth of tumour volume and tumour burden of the normal control group and the skin cancer control group with a significant reduction in the groups of animals treated with 5-FU, compounds 6a, 6h, 6j and 6k: (A) tumour volume; (B) tumour burden.

vitro anticancer activity were evaluated for an *in vivo* anticancer assay. The four best compounds 6a, 6h, 6j and 6k were further screened for *in vivo* anticancer activity. Among these, compound 6h showed the most promising activity compared to 6a, 6j and 6k and emerged as the most potent compound of the series. Structural features like the presence of an ethyl group at the R_1 position and sulphanilamide at the R_2 position in compound 6h were found to be crucial and required for anticancer activity.

In the MCF-7 cell line, compounds 6h, 6j and 6k were found to be more potent than compounds 6a, 6c and 6d, proving the importance of ethyl substitution at the R_1 position. Furthermore, comparison between 6h, 6j and 6k revealed that 6h and 6j were more potent than compound 6k, as compound 6k consisted of an electron withdrawing nitro group on the aromatic amine at the R_2 position, while compounds 6h and 6j consisted of $-SO_2NH_2$ and $-OCH_3$ groups, which are electron donating groups.

In the HEP-3B cell line, compounds 6h, 6i and 6m were found to be more potent than 6a, 6b and 6e. This result again proved the importance of the ethyl group in R_1 substitution, which is present in cases of 6h, 6i and 6m. Further comparisons between 6h, 6i and 6m indicated that substitution at R_2 with a substituted aromatic amine, specifically sulphanilamide, is more favourable in the context of potency compared to the alicyclic or aliphatic amine. This can be proved by the compounds 6h, 6i and 6m, where 6i and 6m were found to be less potent than compound 6h, which consisted of the aromatic amine like sulphanilamide at the R_2 position, while in contrast, compound 6i consisted of piperazine and compound 6m consisted of urea at the R_2 position.

On the other hand, methyl substitution at the R_1 position proved to be active against the DU-145 cell line. These results were in contrast with the other three cell line study results, where an ethyl group at the R_1 position was found to be more effective. This could be proven with compounds 6b and 6d, where compounds 6b and 6d were found to be more potent than 6i and 6k. Further comparisons between compounds 6b and 6d showed that compound 6b was more potent than compound 6d; as compound 6b consisted of piperazine at the R_2 substitution, while in the case of compound 6d, an electron withdrawing group nitro group was present on the aromatic amine at the R_2 position.

compound 6h, compounds with ethyl substitution at the R_1 position (6j, 6k, 6l and 6n) were found to be more potent than compounds 6c, 6d, 6e and 6g, which were substituted with a methyl group at the R_1 position. The R_2 position on the pyrimidine ring was substituted with aliphatic and aromatic amines. Results of *in vitro* anticancer activity revealed that compounds with aromatic amine exhibited more potent anticancer activity compared to aliphatic amines. In the first series, compounds 6a, 6b, 6c and 6d exhibited more potent activity than compounds 6f and 6g, while in the second series, compounds 6h, 6j, 6k and 6l exhibited more potent activity than compounds 6m and 6n. The compounds that showed good *in*
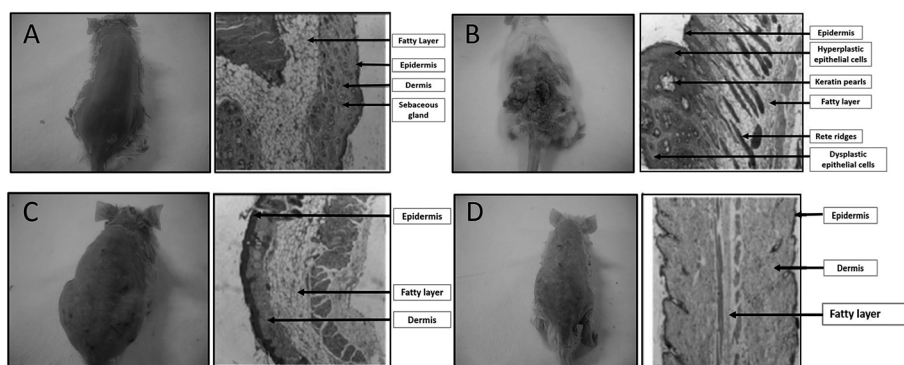

Fig. 6 Images of the caudal region of the skin of the mice and histopathological results of the skin samples: (A) normal control group; (B) skin cancer control group; (C) skin cancer treated with 5-FU; (D) skin cancer treated with compound 6h.

6. Conclusion

Based on pharmacophore-based virtual screening, fourteen novel *N*-phenyl pyrimidine derivatives were designed, synthesised and evaluated against different cancer lines, namely skin cancer (A-375), breast cancer (MCF-7), hepatocellular carcinoma (HEP-3B) and prostate cancer (DU-14). A structure activity relationship study was carried out and proved that an ethyl group at the R_1 and aromatic amines at the R_2 positions of *N*-phenyl pyrimidine were required for activity against skin cancer (A-375). Similarly, in the case of breast cancer (MCF-7), an ethyl group proved effective at the R_1 position together with an electron donating substituted aromatic amine at the R_2 position. In the case of hepatocellular carcinoma (HEP-3B), the R_2 position was found to be favourable for aromatic amines compared to alicyclic or aliphatic amines in combination with an ethyl group at the R_1 position. In contrast, methyl substitution at the R_1 position was found to be more effective against prostate cancer (DU-145) in combination with electron donor amines at the R_2 position. As compounds **6a**, **6h**, **6j** and **6k** revealed good anticancer activity against the skin cancer cell line (A-375), they were further evaluated in the DMBA-induced skin cancer animal model. Among these four derivatives, compound **6h** was found to be best as it treated the tumours completely. The results of the biological screening were quite promising and indicated that compound **6h** was equipotent to **5-FU** and was considered as a good lead compound for future derivatization with a bulky group at the R_1 and aromatic amines at the R_2 positions of *N*-phenyl pyrimidine to design novel compound that should give good anticancer activity against skin cancer.

7. Experimental section

All the reactions were performed using oven dried borosilicate glassware and dry solvents. Precoated silica gel plates (MERCK) were used for TLC to monitor progress of the reaction. A UV chamber and iodine fume chamber were used for the detection of spots on the TLC plates. A REMI Rota-mantle was used for refluxing and stirring the reactions. A rotary vacuum evaporator (BUCHI type) was used for the recovery of the solvents. An IR lamp was used for drying products. Melting points were recorded on VEEGO corporation melting point apparatus. All the compounds were purified by column chromatography, and the purity of all the compounds were checked through the JASCO HPLC instrument. The purity of all the compounds was found to be more than 95%. Mass spectra were recorded on a WATERS mass spectrometer using electron spray ionization (ESI) as the ion source. The ^{1}H and ^{13}C NMR were recorded using tetramethylsilane (TMS) as an internal standard on a BRUKER AVANCE-II 400 MHz spectrometer. Chemical shifts (δ) were reported in ppm, downfield of TMS, and the coupling constants (J) are given in Hz. Single crystal XRD of the most potent compound **6h** was recorded using the RIGAKU SCX mini diffractometer.

The following procedures were used for the synthesis of products **2a** to **5a**:

7.1 Synthesis of methyl-2-cyano-3,3-bis(methylthio)acrylate (2a)

Potassium hydroxide (11.2 g, 0.2 mol) was weighed and dissolved in 5 mL of water, then 15 mL of DMF was added with cooling and stirring was continued for 10 min. In the stirring mixture, methylcyanoacetate (**1a**) (8.8 mL, 0.1 mol) was added, followed by carbon disulphide (6 mL, 0.1 mol). The above mixture was stirred for 1 h at 25 °C and then cooled. DMS (18.9 mL, 0.2 mol) was added drop-wise, maintaining the temperature at 0 °C. The above mixture was added to the crushed ice. A yellow crystalline product of methyl-2-cyano-3,3-bis(methylthio)acrylate (**2a**) was precipitated out, washed with water and dried. The product was recrystallized with *n*-hexane, yielding pure white colour needle-shaped crystals (yield 65.88%, mp 54–56 °C).

7.2 Synthesis of methyl-2-cyano-3-(methylthio)-3-(phenylamino) acrylate (3a)

Compound **2a** (4.06 g, 0.02 mol) and aniline (1.82 mL, 0.02 mol) were refluxed in ethyl alcohol for 2 h. The resulting reaction mixture was cooled in an ice bath. White colour needle-shaped crystals of methyl-2-cyano-3-(methylthio)-3-(phenylamino) acrylate (**3a**) were obtained, filtered and dried (yield 76.19%, mp 62–63 °C).

7.3 Synthesis of methyl-3-(aminomethyleneamino)-2-cyano-3-(phenylamino)acrylate (4a)

Formamidine acetate (2.08 g, 0.02 mol) was added to 1 M ethanolic sodium hydroxide solution. The reaction mixture was allowed to stir for 45 min. Compound **3a** (2.5 g, 0.01 mol) in ethanol was added drop-wise by dropping funnel in to the reaction mixture. The reaction mixture was stirred for 6 h by maintaining the ice-cold condition and added to the crushed ice. A white coloured solid product of methyl-3-(aminomethyleneamino)-2-cyano-3-(phenylamino)acrylate (**4a**) was precipitated out, filtered and dried (yield 75.62%, mp 69–71 °C).

7.4 Synthesis of methyl-4-chloro-6-(phenylamino)pyrimidine-5-carboxylate (5a)

Compound **4a** (4.8 g, 0.02 mol) was added, with stirring, to 25 mL of saturated solution of 1,4-dioxane with dry HCl gas. The stream of dry HCl gas was passed under the same reaction mixture for 24 h. The reaction mixture was added to the crushed ice. White precipitates were obtained and were filtered. The obtained compound methyl-4-chloro-6-(phenylamino) pyrimidine-5-carboxylate (**5a**) was again dissolved in the saturated bicarbonate solution to neutralize the excessive acid. The compound was filtered and dried (yield 66.37%, mp 57–59 °C).

The procedures used for the synthesis of products **2b** to **5b** were as follows:

7.5 Synthesis of ethyl-2-cyano-3,3-bis(methylthio)acrylate (2b)

Same as compound **2a**; instead of methylcyanoacetate, ethyl-cyanoacetate (**1b**) (10.6 mL, 0.1 mol) was used and resulted in a yellow crystalline product **2b**. The product was recrystallized from n-hexane and yielded pure white coloured needle-shaped crystals (yield 63.14%, mp 56–58 °C).

7.6 Synthesis of ethyl-2-cyano-3-(methylthio)-3-(phenylamino)acrylate (3b)

Same as compound **3a**; instead of methyl-2-cyano-3,3-bis(methylthio)acrylate, ethyl-2-cyano-3,3-bis(methylthio)acrylate (**2b**) (2.17 g, 0.01 mol) was used and resulted in a white coloured needle-shaped crystalline product **3b** (yield 51.52%, mp 65–67 °C).

7.7 Synthesis of ethyl-3-(-aminomethyleneamino)-2-cyano-3-(phenylamino)acrylate (4b)

Same as compound **4a**; instead of methyl-2-cyano-3-(methylthio)-3-(phenylamino)acrylate, ethyl-2-cyano-3-(methylthio)-3-(phenylamino)acrylate (**3b**) (2.6 g, 0.01 mol) was used and resulted in a white coloured solid product **4b** (yield 76.92%, mp 70–73 °C).

7.8 Synthesis of ethyl-4-chloro-6-(phenylamino)pyrimidine-5-carboxylate (5b)

Same as compound **5a**; instead of methyl-3-(-aminomethyleneamino)-2-cyano-3-(phenylamino) acrylate, ethyl-3-(aminomethyleneamino)-2-cyano-3-(phenylamino)acrylate (**4b**) (5.16 g, 0.02 mol) was used and resulted in a white coloured solid product **5b** (yield 63.29%, mp 90–92 °C).

The following procedures were used for synthesis of the final step products **6a** to **6n**:

7.9 Synthesis of methyl-4-benezenesulfonamide-6-(phenylamino)pyrimidine-5-carboxylate (6a)

Methyl-4-chloro-6-(phenylamino)pyrimidine-5-carboxylate (**5a**) (2.6 g, 0.01 mol) was mixed with the sulphanilamide (1.7 g, 0.01 mol) in 15 mL of isopropyl alcohol. A catalytic amount of the concentrated HCl was added to the reaction mixture and was refluxed for 6 h and transferred to the crushed ice. White solids of **6a** were precipitated out, filtered and dried (yield 55%, mp 210–212 °C). ^{1}H NMR (400 MHz, DMSO-d_6) δ PPM: 3.96 (s, 3H, –COOC$\underline{H}_3$), 4.50 (s, 2H, 4-SO$_2$N$\underline{H}_2$–C$_6$H$_4$–NH–), 7.13 (d, 2H, J = 8 Hz, Ar-2′,6′-$\underline{H}$), 7.35 (t, 2H, J = 8 Hz, Ar-3′,5′-$\underline{H}$), 7.50 (t, 1H, J = 7.6 Hz, Ar-4′-$\underline{H}$), 7.58 (d, 2H, J = 8 Hz, Ar-2,6-$\underline{H}$), 7.83 (d, 2H, J = 8 Hz, Ar-3,5-$\underline{H}$), 8.26 (s, 1H, C-2 proton of pyrimidine), 10.05 (s, 1H, –N$\underline{H}$–C$_6$H$_5$), 10.31 (s, 1H, 4-SO$_2$NH$_2$–C$_6$H$_4$–N$\underline{H}$–). ^{13}C NMR (400 MHz, DMSO-d_6) δ PPM: 87.16, 121.65, 122.70, 124.05, 126.36, 128.53, 130.43 (2C), 138.48 (2C), 140.90, 141.73, 149.20 (2C), 158.80 (2C), 159, 167.49. Elemental analysis: anal. calcd for C$_{18}$H$_{17}$N$_5$O$_4$S: C, 54.13; H, 4.28; N, 17.67; O, 16.09; S, 8.05. Found: C, 54.17; H, 4.24; N, 17.70; O, 16.13; S, 8.01. MS (EI) m/z for C$_{18}$H$_{17}$N$_5$O$_4$S, found 400.1 MH$^+$.

7.10 Synthesis of methyl-4-(piperazin-1-yl)-6-(phenylamino) pyrimidine-5-carboxylate (6b)

Same as compound **6a**; instead of sulphanilamide, piperazine (0.86 g, 0.01 mol) was used and refluxed for 2 h, yielding a white coloured solid product of **6b** (yield 55%, mp 164–167 °C). ^{1}H NMR (400 MHz, DMSO-d_6) δ PPM: 2.14 (s, 1H, –NH– of piperazine), 2.45 (t, 2H, 2,6-position protons of piperazine), 2.58 (t, 2H, 3,5-position protons of piperazine), 3.68 (s, 3H, –COOC$\underline{H}_3$), 6.93 (d, 2H, J = 8 Hz, Ar-2′,6′-$\underline{H}$), 7.09 (t, 2H, J = 8 Hz, Ar-3′,5′-$\underline{H}$), 7.42 (t, 1H, J = 7.6 Hz, Ar-4′-$\underline{H}$), 8.15 (s, 1H, C-2 proton of pyrimidine), 10.16 (s, 1H, –N$\underline{H}$–C$_6$H$_5$). ^{13}C NMR (400 MHz, DMSO-d_6) δ PPM: 51.68 (2C), 55.17 (2C), 87.16, 113.83, 122.68, 124.51, 128.15 (2C), 129.94 (2C), 131.40, 156.08, 160.17, 167.78. Elemental analysis: anal. calcd for C$_{16}$H$_{19}$N$_5$O$_2$: C, 61.34; H, 6.19; N, 22.27; O, 10.22. Found: C, 61.37; H, 6.14; N, 22.30; O, 10.25. MS (EI) m/z for C$_{16}$H$_{19}$N$_5$O$_2$, found 314.1 MH$^+$.

7.11 Synthesis of methyl-4-(4-methoxyphenylamino)-6-(phenylamino)pyrimidine-5-carboxylate (6c)

Same as compound **6a**; instead of sulphanilamide, 4-methoxyaniline (1.2 g, 0.01 mol) was used and refluxed for 6 h, yielding a white coloured solid product of **6c** (yield 95%, mp 145–147 °C). ^{1}H NMR (400 MHz, DMSO-d_6) δ PPM: 3.86 (s, 3H, 4-OC$\underline{H}_3$–C$_6$H$_4$–NH–), 3.96 (s, 3H, –COOC$\underline{H}_3$), 6.91 (d, 2H, J = 8 Hz, Ar-2′,6′-$\underline{H}$), 7.28 (t, 2H, J = 8 Hz, Ar-3′,5′-$\underline{H}$), 7.35 (t, 1H, J = 8 Hz, Ar-4′-$\underline{H}$), 7.42 (d, 2H, J = 8 Hz, Ar-3,5-$\underline{H}$), 7.60 (d, 2H, J = 8 Hz, Ar-2,6-$\underline{H}$), 8.15 (s, 1H, C-2 proton of pyrimidine), 9.92 (s, 1H, –N$\underline{H}$–C$_6$H$_5$), 10.16 (s, 1H, 4-OCH$_3$–C$_6$H$_4$–N$\underline{H}$–). ^{13}C NMR (400 MHz, DMSO-d_6) δ PPM: 16.47, 76.28, 85.80, 113.63, 117.63, 122.66, 123.78, 124.96 (2C), 126.51 (2C), 128.15, 131.40 (2C), 138.36 (2C), 156.08, 158.94, 160.17. Elemental analysis: anal. calcd for C$_{19}$H$_{18}$N$_4$O$_3$: C, 65.12; H, 5.19; N, 15.90; O, 13.2. Found C, 65.17; H, 5.15; N, 15.93; O, 13.7. MS (EI) m/z for C$_{19}$H$_{18}$N$_4$O$_3$, found 351.1 MH$^+$.

7.12 Synthesis of methyl-4-(4-nitrophenylamino)-6-(phenylamino)pyrimidine-5-carboxylate (6d)

Same as compound (**6a**); instead of sulphanilamide, 4-nitroaniline (1.4 g, 0.01 mol) was used and refluxed for 6 h, yielding a yellow coloured solid product of **6d** (yield 95%, mp 160–162 °C). ^{1}H NMR (400 MHz, DMSO-d_6) δ PPM: 3.67 (s, 3H, –COOC$\underline{H}_3$), 6.14 (d, 2H, J = 8 Hz, Ar-2′,6′-$\underline{H}$), 6.95 (t, 2H, J = 8 Hz, Ar-3′,5′-$\underline{H}$), 6.96 (t, 1H, J = 8 Hz, Ar-4′-$\underline{H}$), 7.51 (d, 2H, J = 8 Hz, Ar-2,6-$\underline{H}$), 7.65 (d, 2H, J = 8 Hz, Ar-3,5-$\underline{H}$), 8.19 (s, 1H, C-2 proton of pyrimidine), 10.03 (s, 1H, –N$\underline{H}$–C$_6$H$_5$), 10.09 (s, 1H, 4-NO$_2$–C$_6$H$_4$–N$\underline{H}$–). ^{13}C NMR (400 MHz, DMSO-d_6) δ PPM: 14.10, 62.35, 76.23, 125.36, 128.52 (2C), 130.11 (2C), 130.81, 134.22 (2C), 136.31 (2C), 136.35, 137.10, 149.10, 155.85, 169.85. Elemental analysis: anal. calcd for C$_{18}$H$_{15}$N$_5$O$_4$: C, 59.19; H, 4.17, N, 19.16; O, 17.2. Found: C, 59.16; H, 4.15; N, 19.20; O, 17.4. MS (EI) m/z for C$_{18}$H$_{15}$N$_5$O$_4$, found 366.3 MH$^+$.

7.13 Synthesis of methyl-4-(4-toludino-6-(phenylamino) pyrimidine-5-carboxylate (6e)

Same as compound (**6a**); instead of sulphanilamide, 4-methylaniline (1.07 g, 0.01 mol) was used and refluxed for 6 h, yielding a white coloured solid product of **6e** (yield 78%, mp 195–197 °C). ^{1}H NMR (400 MHz, DMSO-d_6) δ PPM: 3.41 (s, 3H, 4-C$\underline{H}_3$–C$_6$H$_4$–NH–), 3.67 (s, 3H, –COOC$\underline{H}_3$), 7.10 (d, 2H, J = 8 Hz, Ar-2′,6′-$\underline{H}$), 7.14 (t, 2H, J = 8 Hz, Ar-3′,5′-$\underline{H}$), 7.27 (t, 1H, J = 8 Hz, Ar-4′-H), 7.36 (d, 2H, J = 6.6 Hz, Ar-2,6-H), 7.43 (d, 2H, J = 8 Hz, Ar-3,5-H), 8.19 (s, 1H, C-2 proton of pyrimidine), 9.06 (s, 1H, –N$\underline{H}$–C$_6$H$_5$), 9.14 (s, 1H, 4-CH$_3$–C$_6$H$_4$–N$\underline{H}$–). ^{13}C NMR (400 MHz, DMSO-d_6) δ PPM: 20.37, 51.69, 85.69, 117.66, 120.27, 121.70, 122.80 (2C), 123.88 (2C), 126.51, 128.67, 130.92 (2C), 133.02 (2C), 138.40,

160.14, 169.91. Elemental analysis: anal. calcd for $C_{19}H_{18}N_4O_2$: C, 68.19; H, 5.45; N, 16.49; O, 9.71. Found: C, 68.22; H, 5.41; N, 16.46; O, 9.67. MS (EI) m/z for $C_{19}H_{18}N_4O_2$, found 334 MH$^+$.

7.14 Synthesis of methyl-4-ureido-6-(phenylamino) pyrimidine-5-carboxylate (6f)

Same as compound (6a); instead of sulphanilamide, urea (0.6 g, 0.01 mol) was used and refluxed for 2 h, yielding a white coloured solid product of 6f (yield 98%, mp 200–202 °C). ^{1}H NMR (400 MHz, DMSO-d_6) δ PPM: 3.67 (s, 3H, –COOCH$_3$), 7.11 (s, 2H, –NH–CO–NH$_2$), 7.27 (t, 2H, J = 8 Hz, Ar-3′,5′-H), 7.36 (d, 2H, J = 8 Hz, Ar-2′,6′-H), 7.41 (t, 1H, J = 8 Hz, Ar-4′-H), 7.61 (s, 1H, –NH–C$_6$H$_5$), 8.09 (s, 1H, C-2 proton of pyrimidine), 8.22 (s, 1H, –NH–CO–NH$_2$). ^{13}C NMR (400 MHz, DMSO-d_6) δ PPM: 51.43, 76.19, 117.68, 123.30, 126.49 (2C), 128.68 (2C), 129.25, 138.46, 152.19, 165.84, 169.12. Elemental analysis: anal. calcd for $C_{13}H_{13}N_5O_3$: C, 54.17; H, 4.32; N, 24.27; O, 16.28. Found: C, 54.20; H, 4.34; N, 24.30; O, 16.25. MS (EI) m/z for $C_{13}H_{13}N_5O_3$, found 288.2 MH$^+$.

7.15 Synthesis of methyl-4-thioureido-6-(phenylamino) pyrimidine-5-carboxylate (6g)

Same as compound (6a); instead of sulphanilamide, thiourea (0.76 g, 0.01 mol) was used and refluxed for 2 h, yielding a white coloured solid product of 6g (yield 75.34%, mp 214–216 °C). ^{1}H NMR (400 MHz, DMSO-d_6) δ PPM: 3.26 (s, 3H, –COOCH$_3$), 6.46 (s, 2H, –NH–CS–NH$_2$), 7.10 (d, 2H, J = 8 Hz, Ar-2′,6′-H), 7.88 (t, 2H, J = 8 Hz, Ar-3′,5′-H), 8.18 (t, 1H, J = 8 Hz, Ar-4′-H), 8.31 (s, 1H, –NH–C$_6$H$_5$), 8.37 (s, 1H, C-2 proton of pyrimidine), 9.05 (s, 1H, –NH–CS–NH$_2$). ^{13}C NMR (400 MHz, DMSO-d_6) δ PPM: 75.30, 113.10, 115.56, 119.10, 120.81, 125.10 (2C), 129.15 (2C), 133.16, 161.10, 163.14, 170.07. Elemental analysis: anal. calcd for $C_{13}H_{13}N_5O_2S$: C, 51.35; H, 4.33; N, 23.03; O, 10.49; S, 10.59. Found: C, 51.32, H, 4.30, N, 23.08, O, 10.45, S, 10.56, MS (EI) m/z for $C_{13}H_{13}N_5O_2S$, found 304.4 MH$^+$.

7.16 Synthesis of ethyl-4-benzenesulfonamide-6-(phenylamino)pyrimidine-5-carboxylate (6h)

Ethyl-4-chloro-6-(phenylamino)pyrimidine-5-carboxylate (5b) (2.7 g, 0.01 mol) was mixed with the sulphanilamide (1.72 g, 0.01 mol) in 15 mL of isopropyl alcohol. A catalytic amount of the concentrated HCl was added to the reaction mixture and was refluxed for 6 h and then transferred to the crushed ice. A white solid of 6h was precipitated out, filtered and dried (yield 49%, mp 214–218 °C). ^{1}H NMR (400 MHz, DMSO-d_6) δ PPM: 1.20 (t, 3H, J = 6.79 Hz, –COOCH$_2$CH$_3$), 3.40 (s, 2H, 4-SO$_2$NH$_2$–C$_6$H$_4$–NH–), 4.13 (q, 2H, J = 6.8 Hz, –COOCH$_2$CH$_3$), 7.12 (d, 2H, J = 6.99 Hz, Ar-2′,6′-H), 7.33 (t, 2H, J = 6.99 Hz, Ar-3′,5′-H), 7.61 (t, 1H, J = 8 Hz, Ar-4′-H), 7.81 (d, 2H, J = 9.33 Hz, Ar-2,6-H), 7.84 (d, 2H, J = 8 Hz, Ar-3,6-H), 8.31 (s, 1H, C-2 proton of pyrimidine), 10.07 (s, 1H, –NH–C$_6$H$_5$), 10.32 (s, 1H, 4-SO$_2$NH$_2$–C$_6$H$_4$–NH–). ^{13}C NMR (400 MHz, DMSO-d_6) δ PPM: 13.88, 62.11, 87.36, 121.20, 122.20, 123.91, 126.46 (2C), 128.62 (2C), 129.23, 138.37, 138.43 (2C), 141.71 (2C), 158.81, 159.72, 166.98. Elemental analysis: anal. calcd for $C_{19}H_{19}N_5O_4S$: C, 55.29; H, 4.47; N, 16.39; O, 15.54; S, 7.59. Found: C, 55.25; H, 4.43; N, 16.35; O,

15.57; S, 7.56. MS (EI) m/z for $C_{19}H_{19}N_5O_4S$, found 414.2 MH$^+$. X-crystallographic structure of this compound is shown in (Fig. 2).

7.17 Synthesis of ethyl-4-(piperazin-1-yl)-6-(phenylamino) pyrimidine-5-carboxylate (6i)

Same as compound 6h; instead of sulphanilamide, piperazine (0.86 g, 0.01 mol) was used and refluxed for 2 h, yielding a white coloured solid product of 6i (yield 49.2%, mp 179–182 °C). ^{1}H NMR (400 MHz, DMSO-d_6) δ PPM: 1.30 (t, J = 6.8 Hz, 3H, –COOCH$_2$CH$_3$), 2.60 (t, 2H, J = 8 Hz, 2,6-position protons of piperazine), 2.65 (t, 2H, J = 8 Hz, 3,5-position protons of piperazine), 3.35 (s, 1H, –NH– of piperazine), 4.25 (q, 2H, J = 6.8 Hz, –COOCH$_2$CH$_3$), 6.40 (d, 2H, J = 8 Hz, Ar-2′,6′-H), 7.29 (t, 2H, J = 8 Hz, Ar-3′,5′-H), 7.35 (t, 1H, J = 8 Hz, Ar-4′-H), 8.27 (s, 1H, C-2 proton of pyrimidine), 8.32 (s, 1H, –NH–C$_6$H$_5$). ^{13}C NMR (400 MHz, DMSO-d_6) δ PPM: 14.11, 45.91 (2C), 52.85 (2C), 60.78, 115.25, 117.37, 118.25, 119.33 (2C), 120.34 (2C), 129.33, 154.22, 166.46, 169.30. Elemental analysis: anal. calcd for $C_{17}H_{21}N_5O_2$: C, 62.16, H, 6.34, N, 21.39, O, 9.47. Found: C, 62.20; H, 6.37; N, 21.36; O, 9.50. MS (EI) m/z for $C_{17}H_{21}N_5O_2$ found 328.12 MH$^+$.

7.18 Synthesis of ethyl-4-(4-methoxyphenylamino)-6-(phenylamino)pyrimidine-5-carboxylate (6j)

Same as compound 6h; instead of sulphanilamide, 4-methoxyaniline (1.2 g, 0.01 mol) was used and refluxed for 6 h, yielding a white coloured solid product of 6j (yield 78%, mp 185–187 °C). ^{1}H NMR (400 MHz, DMSO-d_6) δ PPM: 1.41 (t, 3H, J = 6.8 Hz, –COOCH$_2$CH$_3$), 3.75 (s, 3H, 4-OCH$_3$–C$_6$H$_4$–NH–), 4.42 (q, 2H, J = 6.8 Hz, –COOCH$_2$CH$_3$), 6.92 (d, 2H, J = 8 Hz, Ar-2′,6′-H), 7.09 (t, 2H, J = 8 Hz, Ar-3′,5′-H), 7.33 (t, 1H, J = 7.6 Hz, Ar-4′-H), 7.46 (d, 2H, J = 8 Hz, Ar-3,5-H), 7.62 (d, 2H, J = 8 Hz, Ar-2,6-H), 8.19 (s, 1H, C-2 proton of pyrimidine), 9.95 (s, 1H, –NH–C$_6$H$_5$), 10.13 (s, 1H, 4-OCH$_3$–C$_6$H$_4$–NH–). ^{13}C NMR (400 MHz, DMSO-d_6) δ PPM: 13.97, 55.18, 60.41, 85.92, 113.72, 122.17, 123.67, 124.00, 124.41 (2C), 128.60 (2C), 129.25, 131.39 (2C), 138.65 (2C), 155.95, 160.02, 167.22. Elemental analysis: anal. calcd for $C_{20}H_{20}N_4O_3$: C, 65.85; H; 5.39; N, 15.47; O, 13.2. Found, C, 65.82, H, 5.37, N, 15.43, O, 13.5. MS (EI) m/z for $C_{20}H_{20}N_4O_3$, found 365.2 MH$^+$.

7.19 Synthesis of ethyl-4-(4-nitrophenylamino)-6-(phenylamino) pyrimidine-5-carboxylate (6k)

Same as compound 6h; instead of sulphanilamide, 4-nitroaniline (1.38 g, 0.01 mol) was used and refluxed for 6 h, yielding a yellow coloured solid product of 6k (yield 74%, mp 150–153 °C). ^{1}H NMR (400 MHz, DMSO-d_6) δ PPM: 1.21 (t, 3H, J = 6.8 Hz, –COOCH$_2$CH$_3$), 4.14 (q, J = 6.8 Hz, 2H, –COOCH$_2$CH$_3$), 6.62 (d, 2H, J = 8 Hz, Ar-2′,6′-H), 6.74 (t, 2H, J = 8 Hz, Ar-3′,5′-H), 7.27 (t, 1H, J = 7.6 Hz, Ar-4′-H), 7.35 (d, 2H, J = 8 Hz, Ar-2,6-H), 7.87 (d, 2H, J = 8 Hz, Ar-3,5-H), 8.01 (s, 1H, C-2 proton of pyrimidine), 10.01 (s, 1H, –NH–C$_6$H$_5$), 11.07 (s, 1H, 4-NO$_2$–C$_6$H$_4$–NH–). ^{13}C NMR (400 MHz, DMSO-d_6) δ PPM: 13.18, 121.46, 122.91 (2C), 124.20, 125.30 (2C), 128.62, 130.37 (2C), 136.62, 136.33 (2C), 139.23, 140.70, 149.72, 158.85, 159.34, 169.95. Elemental analysis: anal. calcd for $C_{19}H_{17}N_5O_4$: C, 60.3; H, 4.64; N, 18.4; O, 16.89. Found: C, 60.8; H, 4.67; N, 18.36; O, 16.85. MS (EI) m/z for $C_{19}H_{17}N_5O_4$, found 380.3 MH$^+$.

7.20 Synthesis of ethyl-4-(4-toluidino)-6-(phenylamino) pyrimidine-5-carboxylate (6l)

Same as compound **6h**; instead of sulphanilamide, 4-toluidine (1.07 g, 0.01 mol) was used and refluxed for 6 h, yielding a white coloured solid product of **6l** (yield 60%, mp 205–208 °C). ^{1}H NMR (400 MHz, DMSO-d_6) δ PPM: 1.29 (t, 3H, J = 6.8 Hz, –COOCH$_2$-CH$_3$), 2.29 (s, 3H, 4-CH$_3$–C$_6$H$_4$–NH–), 3.45 (q, J = 6.8 Hz, 2H, –COOCH$_2$CH$_3$), 6.14 (d, 2H, J = 8 Hz, Ar-2′,6′-H), 6.95 (t, 2H, J = 8 Hz, Ar-3′,5′-H), 7.10 (t, J = 7.6 Hz, 1H, Ar-4′-H), 7.14 (d, J = 8 Hz, 2H, Ar-2,6-H), 7.29 (d, 2H, J = 8 Hz, Ar-3,5-H), 9.15 (s, 1H, C-2 proton of pyrimidine), 10.03 (s, 1H, –NH–C$_6$H$_5$), 10.10 (s, 1H, 4-CH$_3$–C$_6$H$_4$–NH–). ^{13}C NMR (400 MHz, DMSO-d_6) δ PPM: 12.17, 64.12, 78.31, 120.36, 126.52, 129.81 (2C), 132.11, 134.35 (2C), 135.10 (2C), 137.22, 139.31 (2C), 141.61, 144.10, 146.62, 156.85, 170.85. Elemental analysis: anal. calcd for C$_{20}$H$_{20}$N$_4$O$_2$: C, 68.6; H, 5.67; N, 16.03; O, 9.12. Found: C, 68.57; H, 5.70; N, 16.05; O, 9.15. MS (EI) m/z for C$_{20}$H$_{20}$N$_4$O$_2$, found 349.2 MH$^+$.

7.21 Synthesis of ethyl-4-ureido-6-(phenylamino)pyrimidine-5-carboxylate (6m)

Same as compound **6h**; instead of sulphanilamide, urea (0.67 g, 0.01 mol) was used and refluxed for 2 h, yielding a white coloured solid product of **6m** (yield 60.72%, mp 215–217 °C). ^{1}H NMR (400 MHz, DMSO-d_6) δ PPM: 1.21 (t, 3H, J = 6.8 Hz, –COOCH$_2$CH$_3$), 4.10 (q, 2H, J = 6.8 Hz, –COOCH$_2$CH$_3$), 6.38 (s, 2H, –NH–CO–NH$_2$), 7.07 (t, 2H, J = 8 Hz, Ar-3′,5′-H), 7.15 (d, 2H, J = 8 Hz, Ar-2′,6′-H), 7.50 (s, 1H, –NH–C$_6$H$_5$), 7.27 (t, 1H, J = 7.6 Hz, Ar-4′-H), 8.24 (s, 1H, C-2 proton of pyrimidine), 8.41 (s, 1H, –NH–CO–NH$_2$). ^{13}C NMR (400 MHz, DMSO-d_6) δ PPM: 14.10, 60.10, 93.20, 113.10, 115.56, 116.41, 118.10 (2C), 129.15 (2C), 145.46, 156.21, 159.23, 168.12. Elemental analysis: anal. calcd for: C$_{14}$H$_{15}$N$_5$O$_3$, C, 55.57; H, 5.30; N, 23.20; O, 15.47. Found: C, 55.60; H, 5.27; N, 23.23; O, 15.50. MS (EI) m/z for C$_{14}$H$_{15}$N$_5$O$_3$, found 302.2 MH$^+$.

7.22 Synthesis of ethyl-4-thioureido-6-(phenylamino) pyrimidine-5-carboxylate (6n)

Same as compound **6h**; instead of sulphanilamide, thiourea (0.76 g, 0.01 mol) was used and refluxed for 2 h, yielding a white coloured solid product of **6n** (yield 80.14%, mp 219–221 °C). ^{1}H NMR (400 MHz, DMSO-d_6) δ PPM: 1.24 (t, 3H, J = 6.8 Hz, –COOCH$_2$CH$_3$), 4.20 (q, J = 6.8 Hz, 2H, –COOCH$_2$CH$_3$), 6.94 (d, 2H, J = 8 Hz, Ar-2′,6′-H), 7.07 (t, 2H, J = 8 Hz, Ar-3′,5′-H), 7.84 (t, 1H, J = 7.6 Hz, Ar-4′-H), 8.38 (s, 2H, –NH–CS–NH$_2$), 8.47 (s, 1H, C-2 proton of pyrimidine), 8.61 (s, 1H, –NH–C$_6$H$_5$), 9.01 (s, 1H, –NH–CS–NH$_2$). ^{13}C NMR (400 MHz, DMSO-d_6) δ PPM: 10.10, 75.10, 115.66, 120.30, 121.81, 125.10, 129.25 (2C), 130.41 (2C), 134.46, 162.10, 164.84, 170.12. Elemental analysis: anal. calcd for C$_{14}$H$_{15}$N$_5$O$_2$S: C, 52.4; H, 4.73; N, 22.09; O, 10.08; S, 10.3. Found: C, 52.43; H, 4.77; N, 22.04; O, 10.05; S, 10.6, MS (EI) m/z for C$_{14}$H$_{15}$N$_5$O$_2$S, found 318.4 MH$^+$.

7.23 Antiproliferative *in vitro* assay

All the synthesized compounds were evaluated for their anti-cancer activity against A-375 (melanoma), MCF-7 (breast), HEP-3B (hepatoma) and DU-145 (prostate) cancer cell lines. To evaluate the toxic effects of these compounds, they were also screened against a non-cancerous cell line, VERO. For the culturing of all these cell lines, DMEM supplemented with 5% HBSS, penicillin, streptomycin and amphotericin B was utilised.[25] These cell lines were kept in a CO$_2$ incubator, which consisted of a humidified atmosphere of 5% CO$_2$ at 37 °C with 90% humidity. Stock solutions of all the compounds were prepared in 2% DMSO. Different concentrations of these compounds ranging from 100 μM to 1 nM were prepared from the stock solution. Cells were seeded into 96-well plates and incubated for 24 h. After 24 h, different concentrations of compounds were added into the 96-well plate and incubated for 24 h. The effects of the compounds were determined after 24 h by performing MTT assay. This assay was performed by using (3-(4,5-dimethylthiazol-2-yl)-2,5-diphenyltetrazolium bromide) solution (20 mL of 5 mg mL^{-1}). This solution was added to each well and incubation was continued for an additional 3 h, resulting in the formation of dark blue formazan crystals within the cells. These crystals were solubilised by DMSO and their absorbance was estimated with an ELISA plate reader. IC$_{50}$ values of all these compounds were determined by a non-linear regression method by using Graph pad prism 6.

7.24 Induction of skin cancer[26–28]

All the experiments were performed in compliance with the relevant laws and institutional guidelines, and the experimental protocols carried out in present study were permitted by the Institutional Animal Ethics Committee (IAEC) of the Institute of Pharmacy, Nirma University, Ahmedabad, India (vide protocol number: IP/PCHEM/FAC/15-1/022). All the experimental methods are in line with CPCSEA guidelines, Ministry of Environment and Forests, Government of India.

Male Swiss-albino mice weighing 25–30 g were chosen for the study and were maintained under controlled conditions of temperature (25 ± 2 °C), humidity (55 ± 5%) and 12 h light–dark cycle. Male Swiss-albino mice were kept for 1 week acclimatization period. Subsequently the mice were treated with depilatory cream to remove the hairs from the skin, from the lumbar region to the caudal region of their back. After removing the hairs from the skin, the mice were kept for 2 days under standard conditions to check whether the mice were in a hair cycle or not. Mice with no hair growth were chosen for the study and were grouped accordingly. Skin cancer was induced by dimethylbenz(*a*)anthracene (DMBA) and croton oil. 1 mg mL^{-1} concentration of DMBA solution was prepared by dissolving 50 mg of DMBA in 50 mL of acetone. 50 μL of the DMBA solution was sprayed directly on the caudal region of the skin of the mice. Application was made two times a week, while in the 1st week, with a period of 2 days gap between successive doses. A total of 100 μL of DMBA solution was sprayed within a 3 mm^3 area on the caudal skin region of the mice. Two weeks from the initiation of DMBA application, 1% croton oil solution was applied twice a week from the 3rd week to the 16th week. 1% croton oil was prepared by dissolving 1 mL of croton oil in 100 mL of acetone. During this, the treatment with synthesised

compounds was started from the 7th week and continued till the 16th week. Compounds were applied twice a week, followed by the application of croton oil in the disease-induced groups with a gap of 1 h between the two applications.

7.25 Measurement of various parameters[26–28]

At the end of the 16th week, blood was collected by retro-orbital puncture from each mouse and various parameters were evaluated as per the procedure provided in the ESI.† After the collection of blood samples, one animal each of the groups was killed and the caudal region of the skin was excised from the mice and stored in 10% v/v neutral buffered formalin for further histopathological study, as detailed in the ESI.†

Abbreviations used

5-FU	5-Fluorouracil
DMBA	Dimethylbenz(*a*)anthracene
DMEM	Dulbecco's modified eagle's medium
HBSS	Hank's balanced salt solution
GGT	Gamma glutamyl transferase
LDH	Lactate dehydrogenase
CRP	C-reactive protein
MDA	Malondialdehyde
GSH	Reduced glutathione
SOD	Superoxide dismutase

Acknowledgements

References

1 WHO website. (http://www.who.int) assessed on 1 September 2015.

2 A. R. Rao, H. N. Sindhuja, S. M. Dharmesh, K. U. Sankar, R. Sarada and G. A. Ravishankar, Effective Inhibition of Skin Cancer, Tyrosinase, and Antioxidative Properties by Astaxanthin and Astaxanthin Esters from the Green Alga *Haematococcus pluvialis*, *J. Agric. Food Chem.*, 2013, **61**, 3842–3851.

3 M. H. Aziz, S. Reagan-Shaw, J. Wu, B. J. Longley and N. Ahmad, Chemoprevention of skin cancer by grape constituent resveratrol: relevance to human disease?, *FASEB J.*, 2005, **19**, 1193–1195.

4 M. B. Sporn and N. Suh, Chemoprevention of cancer, *Carcinogenesis*, 2000, **21**, 525–530.

5 T. Haque, K. M. Rahman, D. E. Thurston, J. Hadgraft and M. E. Lane, Topical therapies for skin cancer and actinic keratosis, *Eur. J. Pharm. Sci.*, 2015, **77**, 279–289.

6 V. O. Melnikova and H. N. Ananthaswamy, Cellular and molecular events leading to the development of skin cancer, *Mutat. Res.*, 2005, **571**, 91–106.

7 A. Ziegler, A. S. Jonason, D. J. Lefell, J. A. Simonm, S. W. Sharma, J. Kimmelman, L. Remington, T. Jacks and D. E. Brash, Sunburn and p53 in the onset of skin cancer, *Nature*, 1994, **372**, 773–776.

8 H. N. Ananthaswamy, S. M. Loughlin, P. Cox, R. L. Evans, R. L. Ulrich and M. L. Kripke, Sunlight and skin cancer: Inhibition of p53 mutation in UV irradiated mouse by sunscreen, *Nat. Med.*, 1997, **3**, 510–514.

9 M. C. F. Simoes, J. J. S. Sousa and A. A. Pais, Skin cancer and new treatment perspectives: a review, *Cancer Lett.*, 2015, **357**, 8–42.

10 H. N. Bramson, J. Corona, S. T. Davis, S. H. Dickerson, M. Edelstein, S. V. Frye, R. T. Gampe, P. A. Harris, A. Hassell, W. D. Holmes, R. N. Hunter, K. E. Lackey, B. Lovejoy, M. J. Luzzio, V. Montana, W. J. Rocque, D. Rusnak, L. Shewchuk, J. M. Veal, D. H. Walker and L. F. Kuyper, Oxindole-Based Inhibitors of Cyclin-Dependent Kinase 2 (CDK2): Design, Synthesis, Enzymatic Activities, and X-ray Crystallographic Analysis, *J. Med. Chem.*, 2001, **2**, 4339–4358.

11 A. Echalier, K. Bettayeb, Y. Ferandin, O. Lozach, M. Cle, A. Valette, F. Liger, B. Marquet, J. C. Morris, J. Endicott, B. Joseph, L. Meijer, D. The and B. Bettayeb, Meriolins (3-(Pyrimidin-4-yl)-7-azaindoles): Synthesis, Kinase Inhibitory Activity, Cellular Effects, and Structure of a CDK2/Cyclin A/Meriolin Complex, *J. Med. Chem.*, 2008, 737–751.

12 J. H. Alzate-Morales, J. Caballero, A. V. Jague and F. D. G. Nilo, Insights into the Structural Basis of N2 and O6 Substituted Guanine Derivatives as Cyclin-Dependent Kinase 2 (CDK2) Inhibitors: Prediction of the Binding Modes and Potency of the inhibitors by Docking and ONIOM Calculations, *J. Chem. Inf. Model.*, 2009, **49**, 886–899.

13 F. Marchetti, K. L. Sayle, J. Bentley, W. Clegg, N. J. Curtin, J. Endicott, B. T. Golding, R. J. Griffin, K. Haggerty, R. W. Harrington, V. Mesguiche, D. R. Newell, M. E. M. Noble, R. J. Parsons, D. J. Pratt, L. Z. Wang and I. Hardcastle, Structure-based design of 2-arylamino-4-cyclohexylmethoxy-5-nitroso-6-aminopyrimidine inhibitors of cyclin-dependent kinase 2, *Org. Biomol. Chem.*, 2007, **5**, 1577–1585.

14 C. Effects and M. Paprska, 4-Arylazo-3, 5-diamino-1H-pyrazole CDK Inhibitors: SAR Study, Crystal Structure in Complex with CDK2, Selectivity, and Cellular Effects, *J. Med. Chem.*, 2006, 6500–6509.

15 N. M. Mascarenhas and N. Ghoshal, An efficient tool for identifying inhibitors based on 3D-QSAR and docking using feature-shape pharmacophore of biologically active conformation: A case study with CDK2/CyclinA, *Eur. J. Med. Chem.*, 2008, **43**, 2807–2818.

16 P. Yang, K. Z. Myint, Q. Tong, R. Feng, H. Cao, A. A. Almehizia, M. H. Alqarni, L. Wang, P. Bartlow, Y. Gao, J. Gertsch, J. Teramachi, N. Kurihara, G. D. Roodman, T. Cheng and X. Xie, Lead Discovery, Chemistry Optimization, and Biological Evaluation Studies of Novel Biamide Derivatives as CB2 Receptor Inverse Agonists and Osteoclast Inhibitors, *J. Med. Chem.*, 2012, **55**, 9973–9987.

17 X. Zhaoa, M. Yuan, B. Haung and L. Zhu, Ligand-Based Pharmacophore Model of N-Aryl and N-Heteroaryl Piperazine 1A-Adrenoceptors Antagonists using GALAHAD, *J. Mol. Graphics Modell.*, 2010, **29**, 126–136.

18 P. Athri, T. Wenzler, R. Tidwell, S. M. Bakunova and W. D. Wilson, Pharmacophore Model for Pentamidine Analogs Active Against Plasmodium Falciparum, *Eur. J. Med. Chem.*, 2010, **18**, 6147–6151.

19 J. Cabellero, 3D-QSAR (CoMFA and CoMSIA) and Pharmacophore (GALAHAD) Studies on the Differential Inhibition of Aldose by Flavonid Compounds, *J. Mol. Graphics Modell.*, 2010, 435–476.

20 X. Dong, X. Zhou, H. Jing, J. Chen, T. Liu, B. Yang, Q. He and Y. Hu, Pharmacophore Identification, Virtual Screening, and Biological Evaluation of Prenylated Flavonoids Derivatives as PKB/Akt1 Inhibitors, *Eur. J. Med. Chem.*, 2011, 1023–1066.

21 H. Bhatt, P. Pannecouque and P. Patel, Discovery of HIV-1 Integrase Inhibitors:Pharmacophore Mapping, Virtual Screening, Molecular Docking, In silico ADMET Studies, *Chem. Biol. Drug Des.*, 2013, 1–13.

22 V. Vyas, M. Ghate and A. Goel, Pharmacophore Modeling, Virtual Screening, Docking and In Silico ADMET Analysis of Protein Kinase B (PKB) Inhibitors, *J. Mol. Graphics Modell.*, 2013, **42**, 17–25.

23 S. Krishna, D. K. Singh, S. Meena, D. Datta, M. I. Siddiqi and D. Banerjee, Pharmacophore-Based Screening and Identification of Novel Human Ligase I Inhibitors with Potential Anticancer Activity, *J. Chem. Inf. Model.*, 2014, **54**, 781.

24 M. T. Chhabria, H. G. Bhatt, H. G. Raval and P. M. Oza, Synthesis and biological evaluation of some 5-ethoxycarbonyl-6-isopropylamino-4-(substitutedphenyl) aminopyrimidines as potent analgesic and anti-inflammatory agents, *Bioorg. Med. Chem. Lett.*, 2007, **17**, 1022–1024.

25 V. K. Vyas, B. Variya and M. D. Ghate, Design, synthesis and pharmacological evaluation of novel substituted quinoline-2-carboxamide derivatives as human dihydroorotate dehydrogenase (hDHODH) inhibitors and anticancer agents, *Eur. J. Med. Chem.*, 2014, **82**, 385–393.

26 C. H. Hsu, Y. S. Ho, C. S. Lai, S. C. Hsieh, L. H. Chen, E. Lin, C. T. Ho and M. H. Pan, Hexahydro-β-Acids Potently Inhibit 12-O-Tetradecanoylphorbol 13-Acetate-Induced Skin Inflammation and Tumor Promotion in Mice, *J. Agric. Food Chem.*, 2013, **61**, 11541–11549.

27 H. M. Chen, Y. H. Lee and Y. J. Wang, ROS-Triggered Signaling Pathways Involved in the Cytotoxicity and Tumor Promotion Effects of Pentachlorophenol and Tetrachlorohydroquinone, *Chem. Res. Toxicol.*, 2015, **28**, 339–350.

28 V. Subramanian, B. Venkatesan, A. Tumala and E. Vellaichamy, Topical application of Gallic acid suppresses the 7,12-DMBA/Croton oil induced two-step skin carcinogenesis by modulating anti-oxidants and MMP-2/MMP-9 in Swiss albino mice, *Food Chem. Toxicol.*, 2014, **66**, 44–55.